

MODELLING THE BEHAVIOUR OF REINFORCED CONCRETE BEAMS STRENGTHENED WITH FRP

P. Neto¹, J. Alfaiate², and J. Vinagre²

¹ Escola Superior de Tecnologia do Barreiro/IPS
Rua Stinville, nº 14, 2830-144 Barreiro
pedro.neto@estbarreiro.ips.pt

² Instituto Superior Técnico/UTL
Av. Rovisco Pais, 1049-001 Lisboa
alfaiate@civil.ist.utl.pt
joao.vinagre@estbarreiro.ips.pt

Keywords: fiber reinforced polymers (FRP), flexural crack, local bond strength, interfacial stress, fracture energy.

Abstract. *The strengthening of reinforced concrete structures with fiber reinforced polymers (FRP) is particularly attractive due to their mechanical properties. The understanding of the premature failure modes is of great importance. Since rupture is frequently found to occur at the interface FRP concrete, there is a clear need to study the nature of the bonding so as to develop techniques to permit its design modeling. The stress distribution in shear test models does not precisely match the one obtained in flexural reinforcement; in the latter, according to various authors [1, 2], in addition to the stresses tangential to the interface, normal stresses are also important. In this paper, a numerical model is presented to describe the behavior of reinforced concrete beams strengthened with FRP. This model is based on previous studies focused both on: i) the distribution of shear stresses at the interface FRP concrete and on ii) the stress concentration at the plate ends in flexural models. Furthermore, the importance of the flexural cracks in the premature rupture of the element is also analyzed. The behavior of reinforced concrete beams strengthened with both FRP laminates and sheets is considered. The FRP epoxy concrete arrangement and the flexural cracks are modeled with interface elements with initial zero thickness, using a discrete approach and a localized damage model. A softening behavior is adopted to simulate the stress transfer along the FRP-concrete interface. The importance of considering the mixed mode of fracture is discussed. Mention is also made to some of the main mathematical models found in the literature.*

1 INTRODUCTION

In recent years, the use of composite materials applied to the external strengthening of concrete structures has increased due to their mechanical properties, ease of application and high strength-to-weight ratio. The major problems found with this technique are the local failure modes. Results from experiments reveal that the strength of a glued concrete-FRP (fiber reinforced polymers) bond is determined, in most cases, by the high interfacial stresses. Thus, there is a clear need to study the nature of the bonding as well as developing techniques to permit its design modeling and an accurate quantification of the adherence between the concrete and the reinforcing material.

The stress distribution on pure shear test models does not precisely match the one obtained in bending reinforcement; in the latter, according to various authors [1, 2, 3, 4], in addition to the stresses tangential to the interface, normal stresses are also important. The stress concentration at the FRP end can be the cause of the collapse of the strengthened concrete beam. This type of local failure generally occurs along a portion of concrete attached to the epoxy-fiber layers, the latter remaining intact. In these cases, the evaluation of the energy dissipated per unit of cracked surface involves both the fracture energy of concrete in modes I and II, denoted by G_F and G_F^{II} , respectively. Several experimental and numerical tests have been carried out to study mixed-mode fracture. However, the definition of these material parameters is still not well established and the numerical and experimental results reported have often been contradictory. Bazant et al. [5] and Ozbolt et al. [6] proposed for G_F^{II} values about 25 times greater than G_F . Alfaiate et al. [7] performed numerical analyses of notched beams subjected to shear and did not detect any significant differences on the value of the failure load when G_F^{II}/G_F varied from 1 to 100. Such result was confirmed by Gálvez et al. [8], who carried out a similar study. Täljsten [4] performed a set of experimental tests for determining both values of G_F and G_F^{II} . The mode-II fracture energy was determined submitting a concrete specimen to both compression and shear. The values determined for G_F^{II} were found to be 10 times greater than the value of G_F .

The effect of flexural cracks on the interfacial stresses and his contribution to final debonding failure was analyzed by several authors [1, 2, 9]. Shear stresses reveal to have the more significant role. Malek et al. [1] and Wu et al. [2] adopted a linear shear stress-slip model to study the effect of flexural cracks on the interfacial shear stresses. According to Niu et al. [9] a linear bond-slip model does not allow to describe correctly the debonding process, so a bi-linear shear stress-slip model (with softening behavior) was adopted by the authors.

In this paper, special attention is paid to the interfacial stresses due to flexural cracks and to the stress concentration at the FRP end. Subsequent to previous shear-stress studies [10, 11], a numerical model is presented which aims to analyze the stress distribution at the FRP-concrete interface of reinforcement concrete (RC) beam strengthened with FRP. Carbon laminates and sheets are considered. The bond between the FRP and the concrete is modeled using a discrete crack approach based on non-linear fracture mechanics [12]. Interface elements with zero initial thickness are adopted. The shear and peeling stresses developed at these elements are dependent on the relative displacement between the strengthening material and the concrete surface, according to a local constitutive relationship considering softening behavior. The material properties that characterize the interface, namely the shear and peeling stiffness, the cohesion, the tensile strength and the fracture energy in modes I and II, are obtained from previous work [11] and using experimental data from strengthened reinforced concrete bending beams. From the analysis of the results numerically obtained, it is possible to conclude that mode-II fracture plays an important role on these tests and a range of values is proposed for G_F^{II} . It is expected that this work may contribute to a better comprehension of

the stress transfer mechanisms between the concrete and the strengthening material and to clarify the relative importance of some of the local failures modes.

2 EXPERIMENTAL TESTING

In this section, the bending tests conducted by Dias et al. [13] are analyzed. Among the several experimental models tested by Dias et al. [13], the reinforced concrete beams, strengthened with carbon fiber laminates and sheets, without external anchorage systems were considered. Figure 1 illustrates the geometry, the internal and external reinforcing schemes and the boundary conditions, specifically considering FRP laminate. Also the experimental results from concrete beams without external bond reinforcement are analyzed.

The four-point bending beams had a $0.12 \times 0.18\text{m}^2$ cross section, a total length of 1.95m and a span of 1.80m. The unidirectional carbon fibers were glued, by means of resin epoxy, to reinforced concrete beams with a bond length of 1.74m. One layer of $t_f=1.4\text{mm}$ thickness were adopted presenting a $b_f=20\text{mm}$ width and two layer of $t_f=0.111\text{mm}$ thickness were adopted presenting a $b_f=70\text{mm}$ width for laminate and sheet, respectively.

The MBrace HM laminate FRP system was used. The nominal values for the Young's modulus, tensile strength and the ultimate tensile strain of the CFRP were 200GPa, 2200MPa and 1.1%, respectively. The MBrace C1-20 sheet FRP system was used. The nominal values for the Young's modulus, tensile strength and the ultimate tensile strain of the CFRP were 240GPa, 3700MPa and 1.5%, respectively. The adhesive's Young's modulus was 7GPa. Mean values of 47.7MPa, 4.0MPa and 31.1GPa, for the cylinder compressive strength, tensile strength and Young's modulus of concrete, respectively, were obtained experimentally. For the steel, mean values of the yielding stress of 555MPa ($\phi 6$) and 533MPa ($\phi 8$) were found from the tests.

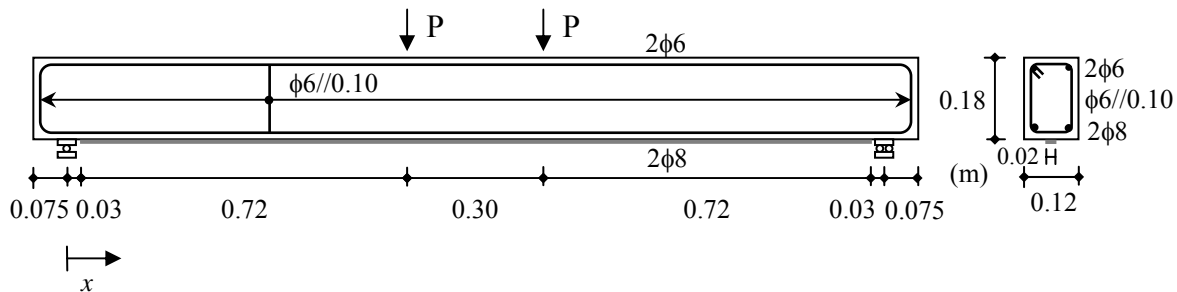


Figure 1: Geometry, reinforcing schemes and boundary conditions, considering FRP laminate.

3 NUMERICAL MODELLING

3.1 Material model

The tensile behavior of the FRP is assumed as linear elastic until failure and an elastic-plastic law is considered for the internal reinforcement.

The concrete is assumed to behave according to an elastic-plastic and isotropic constitutive relationship in compression. In tension, as a continuum, an isotropic linear elastic behavior is adopted for the concrete. At a specific location concrete cracks are considered in order to simulate the loss of tensile strength. In the lower region of the beam these cracks are assumed already open, incapable of stress transfer. In the upper region of the beam interface elements of zero initial thickness are considered, adopting a discrete approach. In this case when the tensile strength is attained a fictitious crack initiates according to the fictitious crack model. A tension cut-off limit surface for mode-I fracture is considered, defined by the tensile strength

of the concrete f_t . This value is considered equal to 4.0MPa, obtained from pull-off tests [13]. The yield function follows an exponential softening flow rule according to equation (1), as shown in Figure 3.

The bond between concrete, resin and CFRP is modeled using interface elements of zero initial thickness and a discrete crack approach. A multi-surface plasticity model is adopted [14, 15]; two limit surfaces are considered: a tension cut-off for mode-I fracture and a Coulomb friction envelope for mode-II failure, as shown in Figure 2. In this figure, the horizontal axis represents the normal stress vector component and the vertical axis represents the tangential stress vector component measured at the interface. The cut-off mode-I is defined by the tensile strength of the concrete. The Coulomb friction envelope is initially characterized by the cohesion coefficient and by the internal friction angle ϕ . Both yield functions follow exponential softening flow rules (Figure 3).

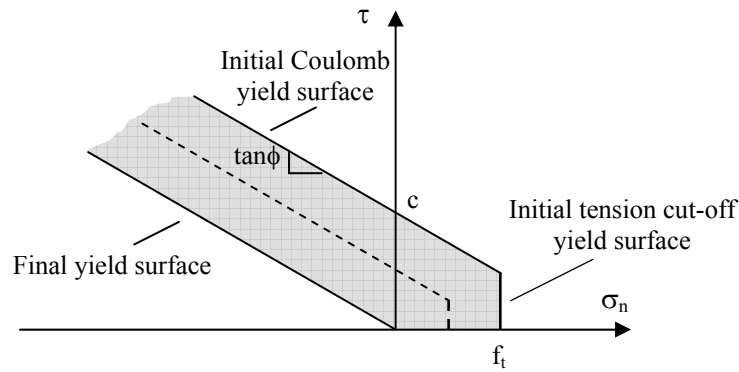


Figure 2: Yield surfaces adopted for the interface.

The tension mode yield function is given by:

$$f_n = \sigma_n - f_t \exp\left(-\frac{f_t}{G_F^I} w\right) \quad (1)$$

where σ_n is the stress vector component measured in the interface. An associated flow rule is considered. The shear mode yield function reads:

$$f_s = |\tau| + \sigma_n \tan \phi - c \cdot \exp\left(-\frac{c}{G_F^{II}} s\right), \quad (2)$$

where τ is the tangential stress vector component measured in the interface. A non-associated flow rule is adopted with a plastic potential g_s given by:

$$g_s = |\tau| + \sigma_n \tan \psi - c, \quad (3)$$

where ψ is the dilatancy angle. An isotropic softening criterion is adopted, meaning that both yield surfaces shrink the same relative amount in the stress space, and both keep the origin (Figure 2).

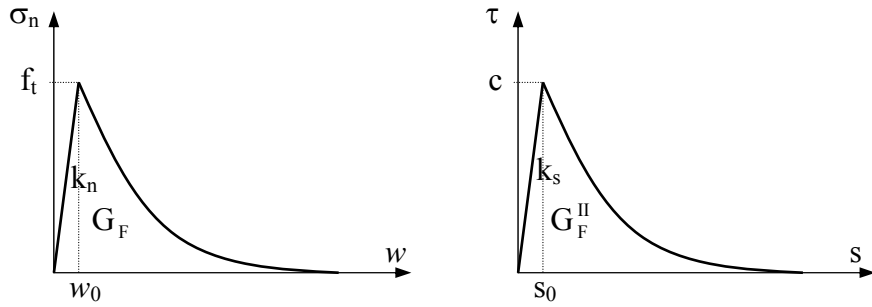


Figure 3 – Normal and tangential constitutive relationships adopted for the interface.

The material parameters characterizing the interface behaviour are: the elastic shear and peeling stiffness, k_s and k_n , respectively, the cohesion c , the tensile strength f_t , and the fracture energies in modes I and II, G_F and G_F^{II} , respectively (area under the curves σ_n-w and $\tau-s$ adopted as shown in Figure 3).

The bond between concrete and steel reinforcement is also modeled using interface elements of zero initial thickness and a discrete crack approach. In this case no softening is considered. Thus, only the interfacial stiffness it is necessary to characterize the constitutive behavior.

3.2 Numerical implementation

The numerical analysis is performed using the finite element method based in a previous model [11]. The elements used for concrete are linear 4-node and 5-node isoparametric. For the strengthening material, 4-node isoparametric elements are adopted (instead of the linear 2-node element used in previous analyses [10]). These elements allow the bending stiffness of the composite to be considered. The bond behavior is modeled by linear interface elements. The specimen response is determined under displacement control, using an incremental and iterative procedure, according to the following algorithm:

1. evaluation of the incremental stiffness matrix of the structure K ;
2. solving of the system of equations $K\Delta u = \Delta \lambda F$, where Δu is the incremental displacement vector, $\Delta \lambda$ is the load increment size and F is the nodal force vector;
3. evaluation of the internal forces F_i . The Newton-Raphson and the arc length methods are used for obtaining convergence towards a solution without unbalanced forces. If equilibrium is not reached within a prescribed tolerance, a new iteration must be performed; otherwise proceed to step 4;
4. update of the total variables, application of another load increment $\Delta \lambda$ and return to step 1.

In some cases, instead of step 3, an explicit integration of the stiffness matrix is adopted.

The symmetric two-dimensional finite element mesh adopted is presented in Figure 4. In the FRP end, a more refined mesh is considered to capture the high stress gradient which is expected in this region (Figure 4). According to observation of Dias et al. work [13] a crack mean spacing of 100mm is assumed. Figure 5 presents the deformation of a RC beam strengthened with FRP, it is possible to note the cracks location and a detail of a crack is shown.

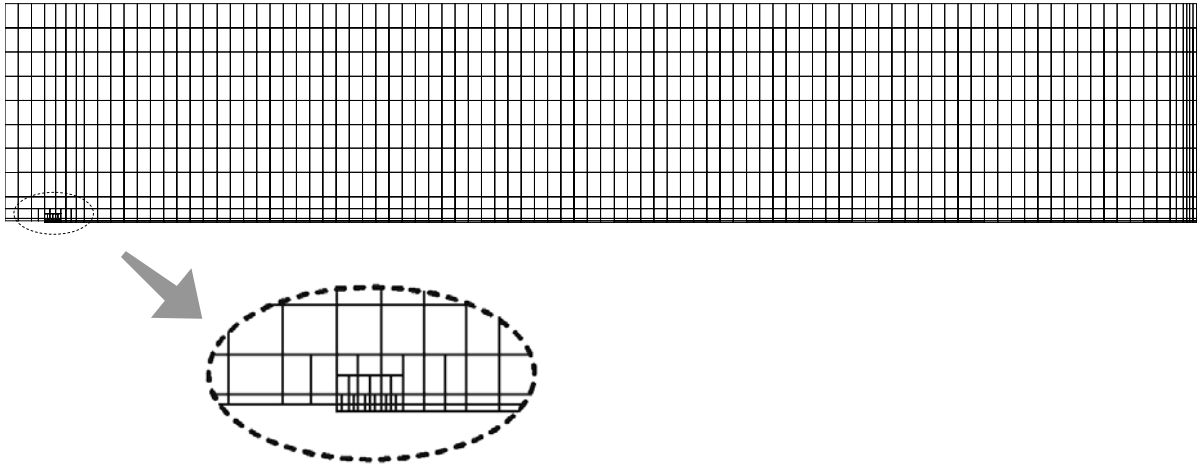


Figure 4 – Finite element mesh adopted and detail at the FRP end.

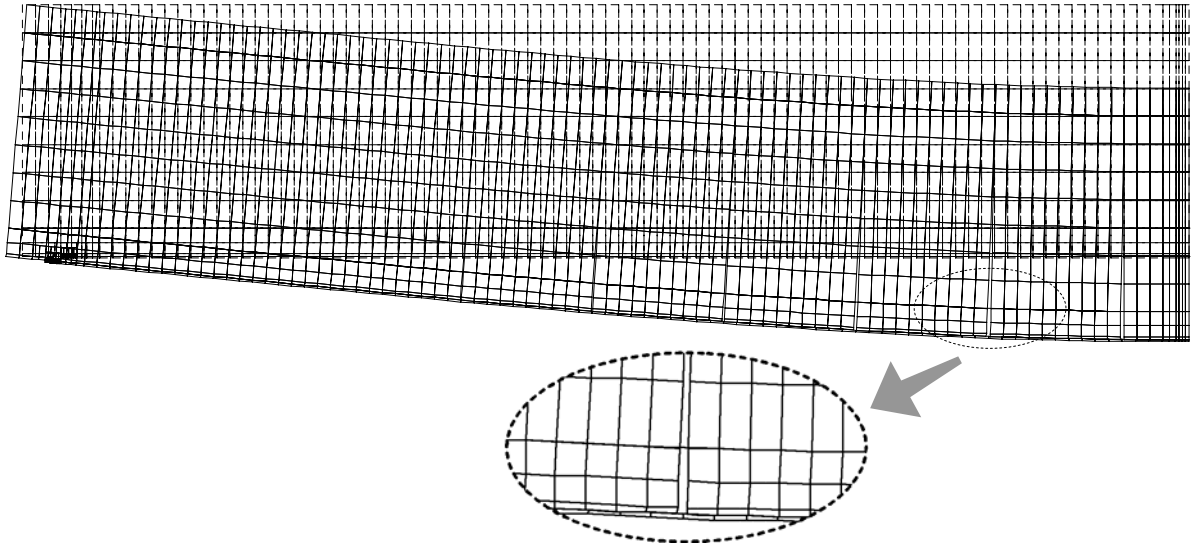


Figure 5 – Deformation of a RC beam strengthened with FRP, detail of a crack and slip at the interface.

3.3 Numerical analysis

As mentioned above, the constitutive relationship of the interface concrete-CFRP is defined by six parameters: the shear and peeling stiffness, the cohesion, the tensile strength and the fracture energy in modes I and II. In the present analysis only debonding failure is acknowledged. In agreement with Malek et al. [1], the stiffness of the interface depends on the adhesive properties according to:

$$k_n = E_a / t_a \quad (4)$$

and

$$k_s = E_a / (2(1 + \nu)t_a), \quad (5)$$

where ν is the Poisson coefficient, E_a is the Young's modulus for adhesive and t_a is the thickness of the adhesive. According to experimental and fabricant data, the values adopted for the calculation of the interface stiffness are: $E_a=7000\text{MPa}$, $\nu=0.3$ and $t_a=1.75\text{mm}$, the latter value

lying between 1.5mm and 2.0mm. Thus, according to equations (4) and (5), the obtained values are $k_n=4000\text{MPa/mm}$ and $k_s=1500\text{MPa/mm}$.

The value for the cohesion is defined taking into account the dependence, mentioned in several works as seen in Neto [16], between this value and the mean value of the concrete tensile strength. A cohesion value $c=7\text{MPa}$ is adopted. The value of $f_t=4.0\text{MPa}$ corresponds to the tests results obtained by Dias et al. [13].

For the mode-II fracture energy, a value $G_F^{\text{II}}=1.5\text{N/mm}$ is defined; this value is predicted taking into account the fact that the concrete used in this study exhibits a higher mechanical strength than the one considered in Neto et al. [10]. Assuming a relation $G_F^{\text{II}}/G_F=10$ [4], we obtain $G_F=0.15\text{ N/mm}$.

The same values are adopted to define the constitutive relationship of the interface concrete-concrete at a flexural crack.

In order to characterize the bond behavior between concrete and internal reinforcing a shear stiffness of 7.8MPa/mm is adopted according to Costa [17], based on a bond model present in Model Code 90 [18]. The peeling stiffness is assumed a high value similar to the other cases.

Next, a numerical study of the behavior of the RC beam strengthened with CFRP is performed. However, in order to calibrate the numerical model, first the beam without external reinforcement is analyzed. Two cases are considered: i) perfect adhesion between concrete-steel reinforcement and ii) a bond-slip relationship between these two materials according to Costa [17]. In the latter case interface elements are adopted. The numerical and experimental results are presented in Figure 6. From the observation of this figure it can be noted that, in case i), only the first part of the numerical curve differs from the experimental one, with a similar response corresponding to steel yielding. In case ii) the curves almost perfectly match and so it can be concluded that the parameters adopted are adequate to continue the analysis.

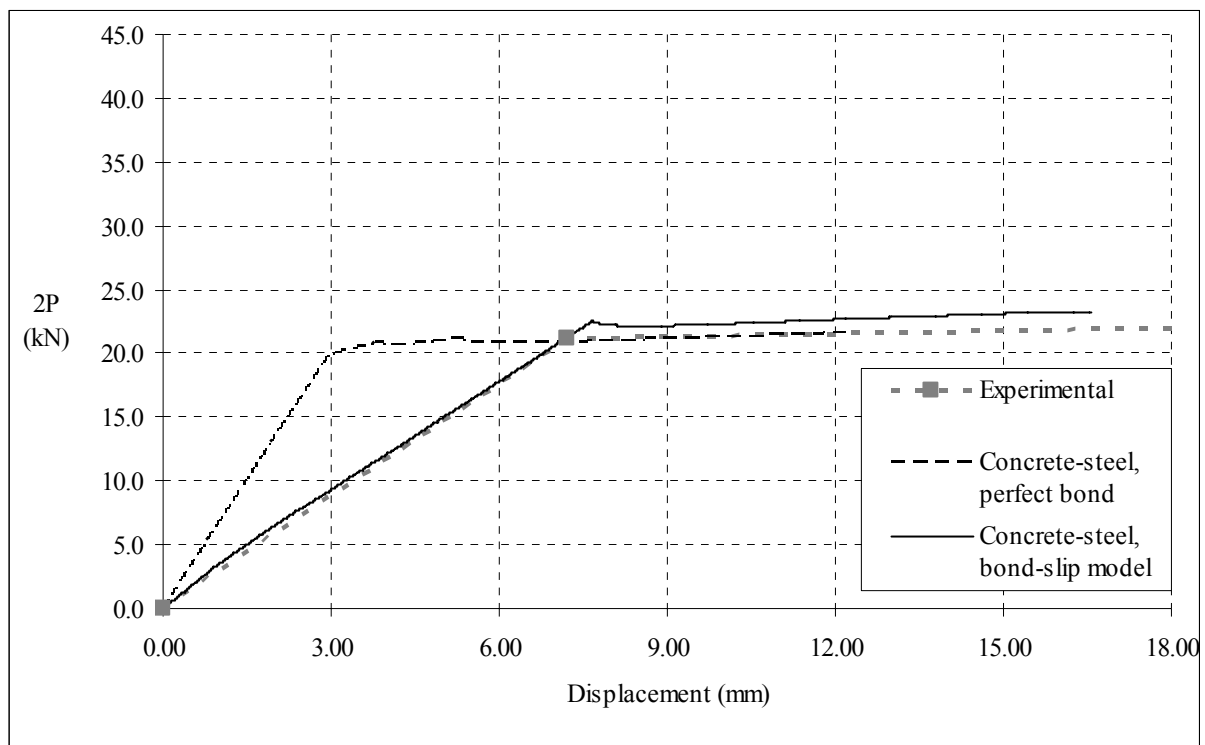


Figure 6 – Response of the reinforced concrete beam without external reinforcement.

Now, the reinforced concrete beam strengthened with FRP laminate response is studied (Figure 7). Interface elements are used to model the connection between concrete and internal reinforcement. Comparing with previous analysis, similar observations can be made, although bigger differences are noted in this case. However, relatively to the last part of the curves, the ratio between experimental and numerical loads is above 90%, which can be considered a good agreement.

The incremental-iterative method revealed problems of convergence due to the softening behaviour. Thus, explicit integration is considered, in spite of the risk of losing numerical precision. However, this aspect is taken into account. Both procedures are compared at the beginning of the analysis, proving to be almost coincident as shown in Figure 7. Beyond this level, attention is paid to the interfacial stresses distribution and to the program's information about the committed error in each step.

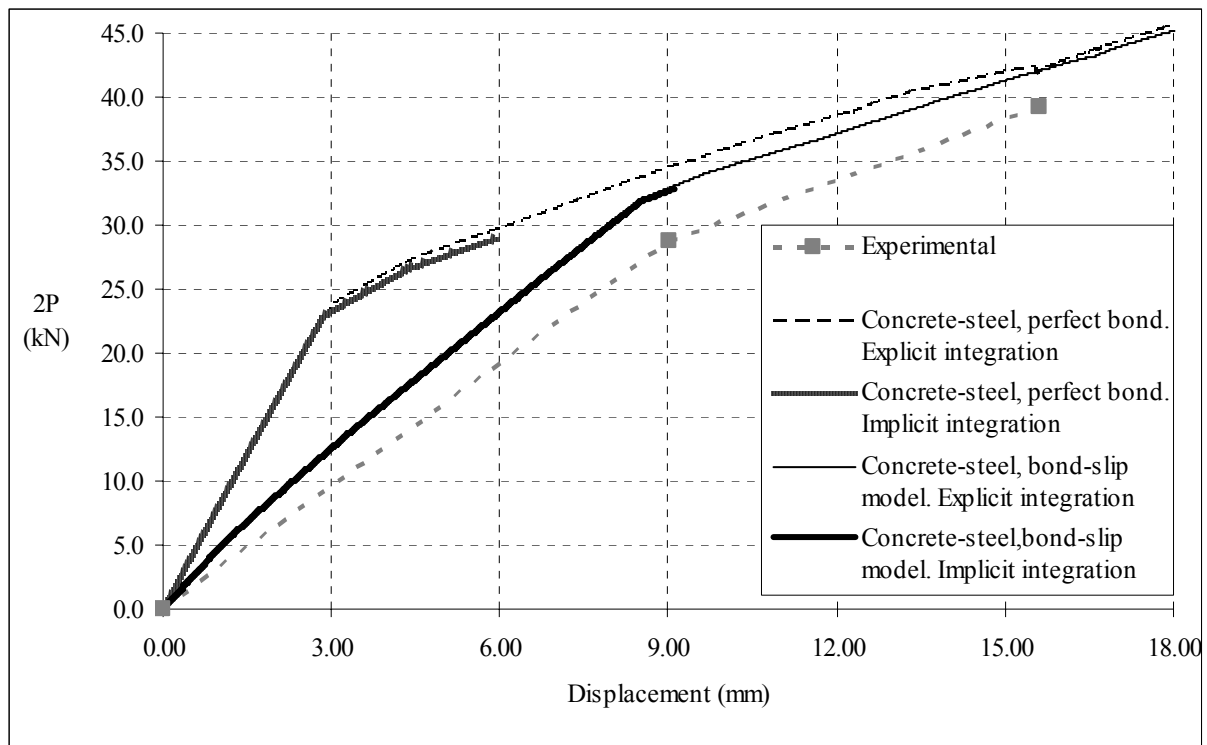


Figure 7 – Response of the reinforced concrete beam strengthened with FRP laminate.

The distribution of interfacial stresses obtained with the finite element method concerning the bond between concrete and CFRP is represented in Figure 8 to Figure 13, where both shear and peeling stresses are shown. According to the type of stress distribution it is possible to distinguish the extremity of the CFRP region from the span region. In the CFRP end the normal stresses appears to have a more important role than at span region where these stresses are compressive stresses. In the composite end region, these stresses are tensile stresses along a small length, becoming compressive stress afterwards, almost vanishing along a length of approximately 10mm. This result is in agreement with Neto et al. [11] and was confirmed by Rabinovich et al. [3], who claims that this distance corresponds to 3-4 times the adhesive thickness. High interfacial stresses can be observed in this region as shown in Figure 21a). The shear stress distribution becomes similar to the one obtained in a pure shear model [10], but between cracks a stress interaction can be noted. The stress superimposition occurs if the crack spacing does not exceed significantly the bond length associated to the maximum force

in the composite, at two adjacent cracks, obtained in a single shear model. This observation is in accordance with the results from a mathematical study carried out by Niu et al. [9]. By applying a simple shear test, the bond length obtained is approximately 260mm [16, 19], greater than the crack spacing.

Analyzing the interfacial stresses along the beam span and at the FRP end, for higher load levels near the maximum load, it can be observed that the debonding due to flexural cracks of concrete is the determinant failure mode. Thus, the local failure mode due to stress concentration at the FRP end is not important here, as noticed by Neto et al. [11]. The small stress concentration found in the FRP end of the beam may be due to the fact that the composite thickness is small enough to mobilize peeling stresses leading to failure. This result seems to be in accordance with the result experimentally observed. The observed behavior in an experimental model, which differs from the numerical model only in the introduction of exterior fixation mechanisms in the extremity of the laminate, was quite similar to the presented one.

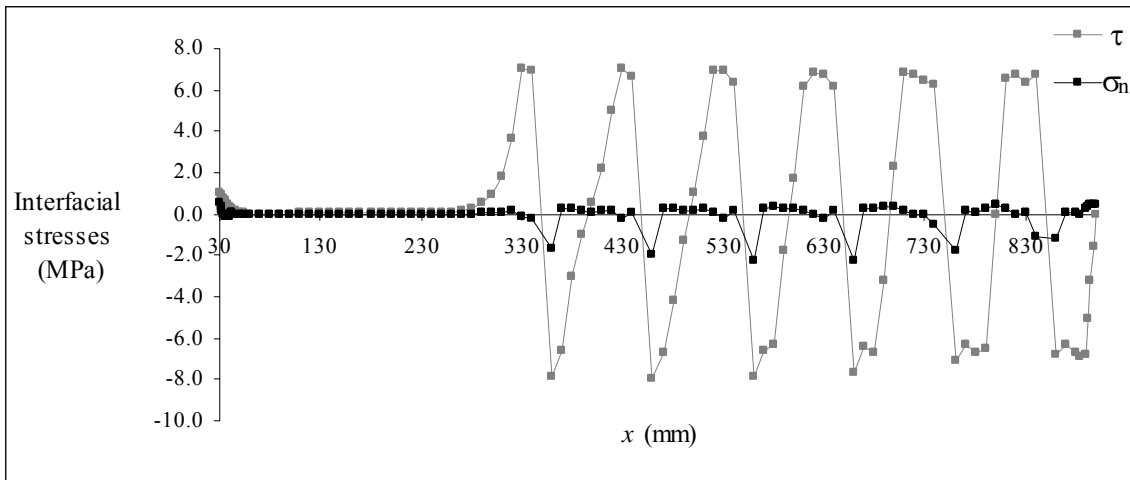


Figure 8 – Interfacial stresses along the beam with $P=5.1\text{kN}$ (laminated).

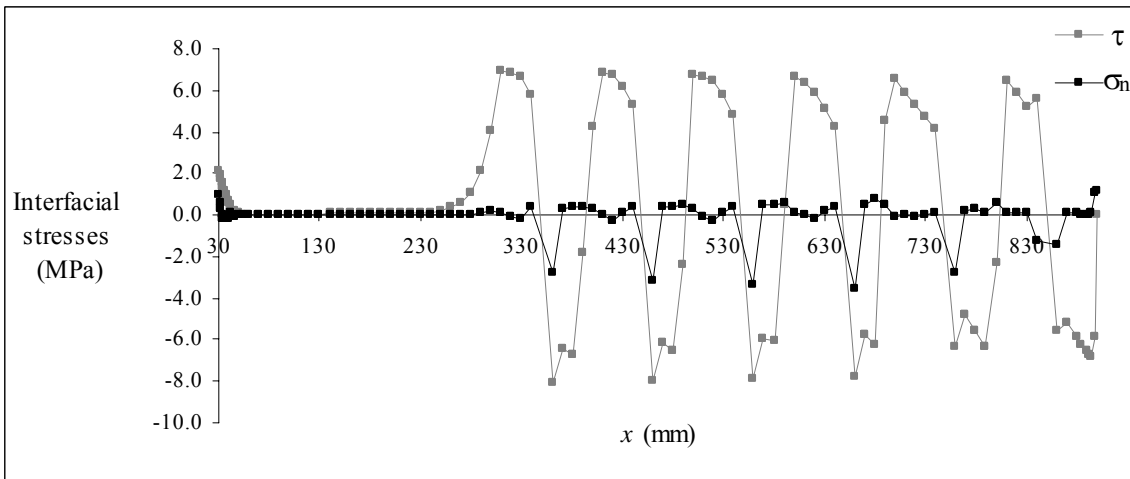


Figure 9 – Interfacial stresses along the beam with $P=10.0\text{kN}$ (laminated).

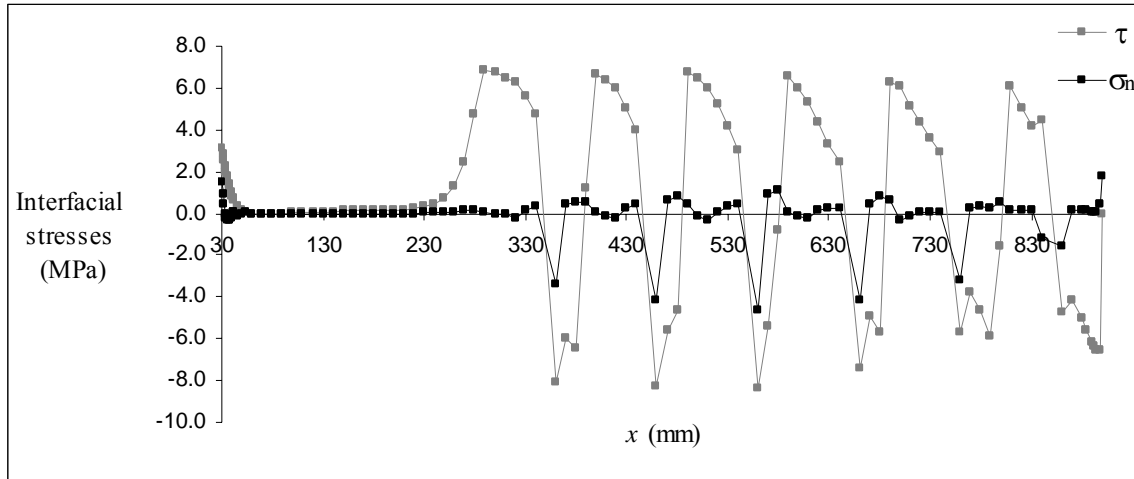


Figure 10 – Interfacial stresses along the beam with $P=14.9\text{kN}$ (laminated).

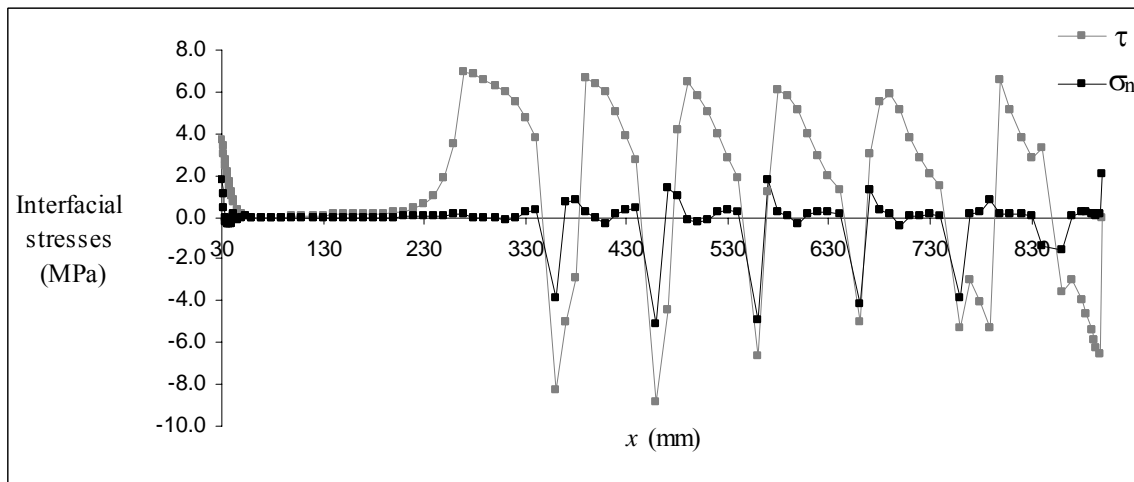


Figure 11 – Interfacial stresses along the beam with $P=18.0\text{kN}$ (laminated).

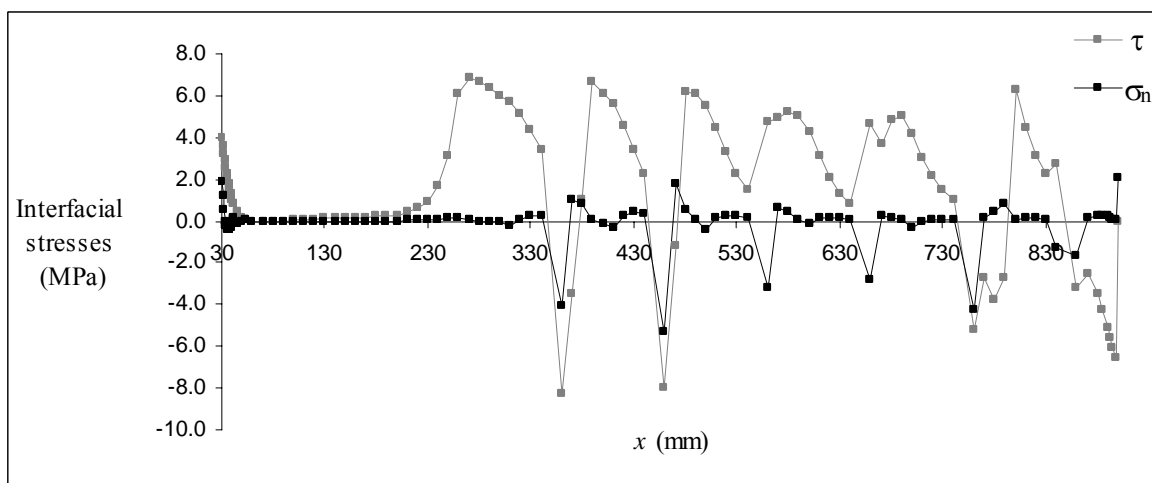


Figure 12 – Interfacial stresses along the beam with $P=19.1\text{kN}$ (laminated).

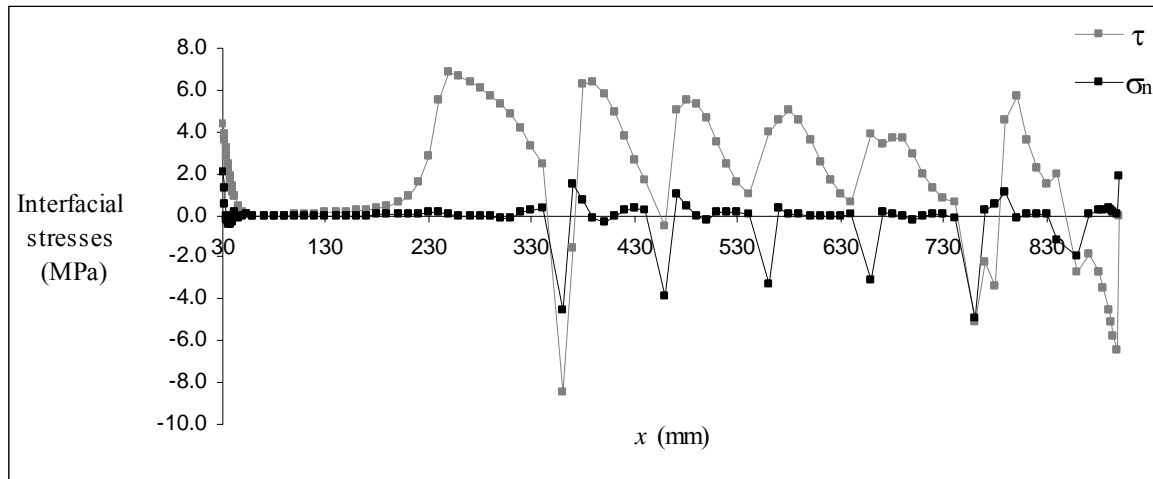


Figure 13 – Interfacial stresses along the beam with $P=21.0\text{kN}$ (laminate).

Taking into account the good agreement observed between numerical and experimental results, indicating the validity of the adopted mathematical model, this study is extended to the case of the RC beam strengthened with FRP sheet. The structure response can be observed in Figure 14 and again relatively good results are obtained.

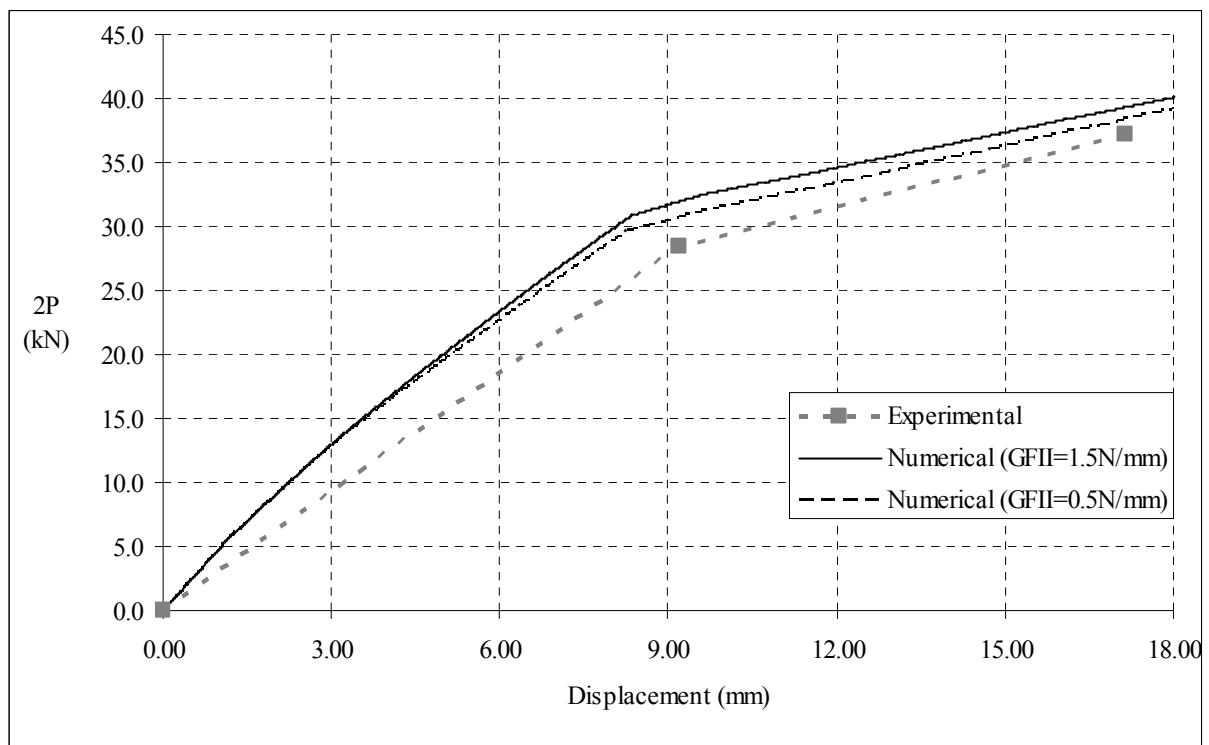


Figure 14 – Response of the reinforced concrete beam strengthened with FRP sheet.

The distribution of interfacial stresses obtained with the finite element method concerning the bond between concrete and CFRP sheet is represented in Figure 15 to Figure 20. The shear stress distribution is similar to the one obtained in the previous model (beam strengthened with carbon laminate) but a lower stress interaction between cracks is noticed. In this

case the effective bond length is about 80mm, considering a shear model [16, 19], less than the crack spacing.

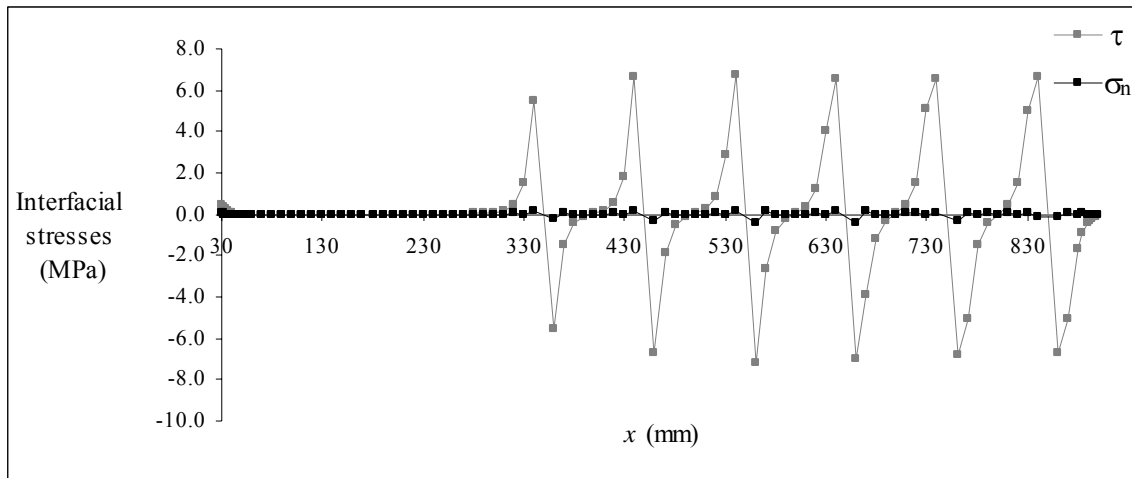


Figure 15 – Interfacial stresses along the beam with $P=4.8\text{kN}$ (sheet).

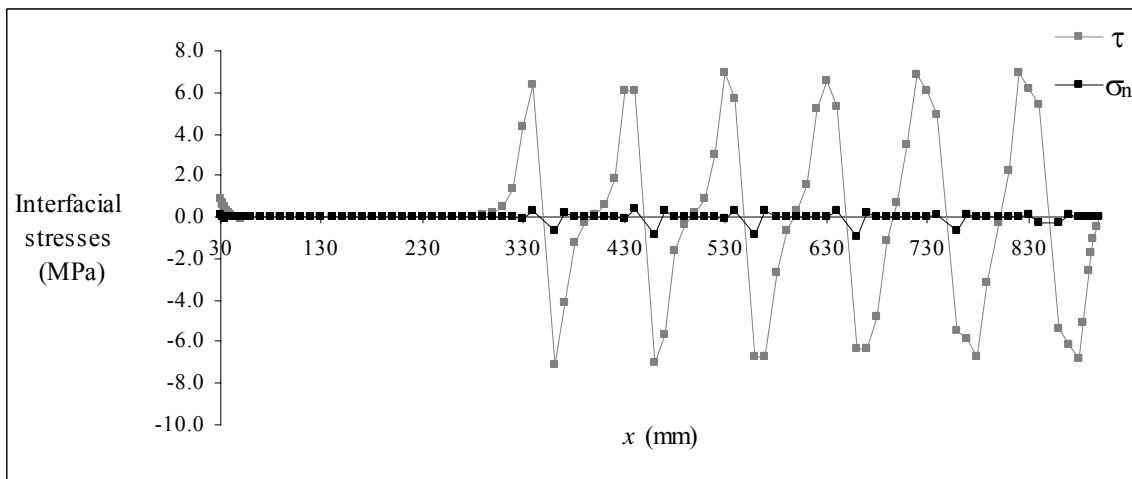


Figure 16 – Interfacial stresses along the beam with $P=9.9\text{kN}$ (sheet).

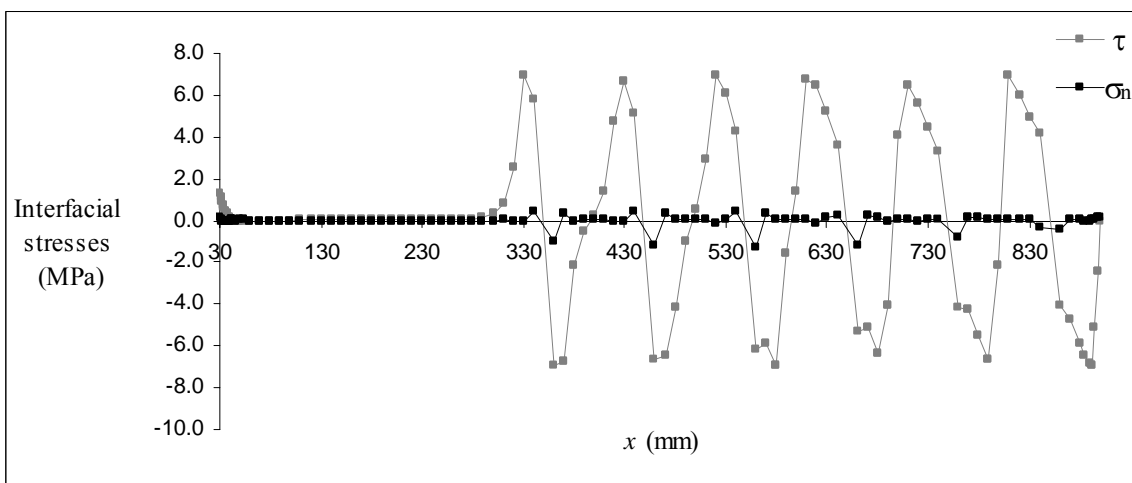


Figure 17 – Interfacial stresses along the beam with $P=15.1\text{kN}$ (sheet).

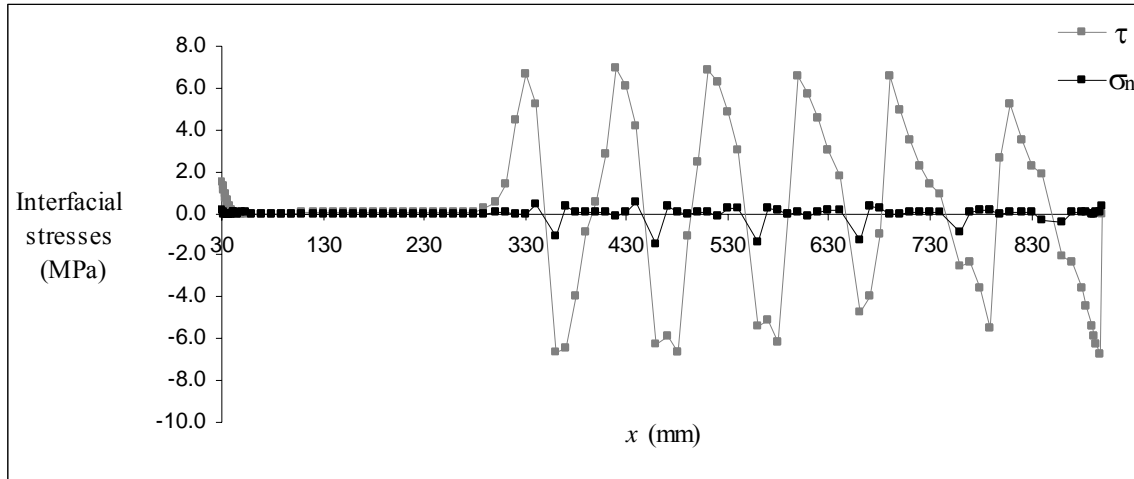


Figure 18 – Interfacial stresses along the beam with $P=18.1\text{kN}$ (sheet).

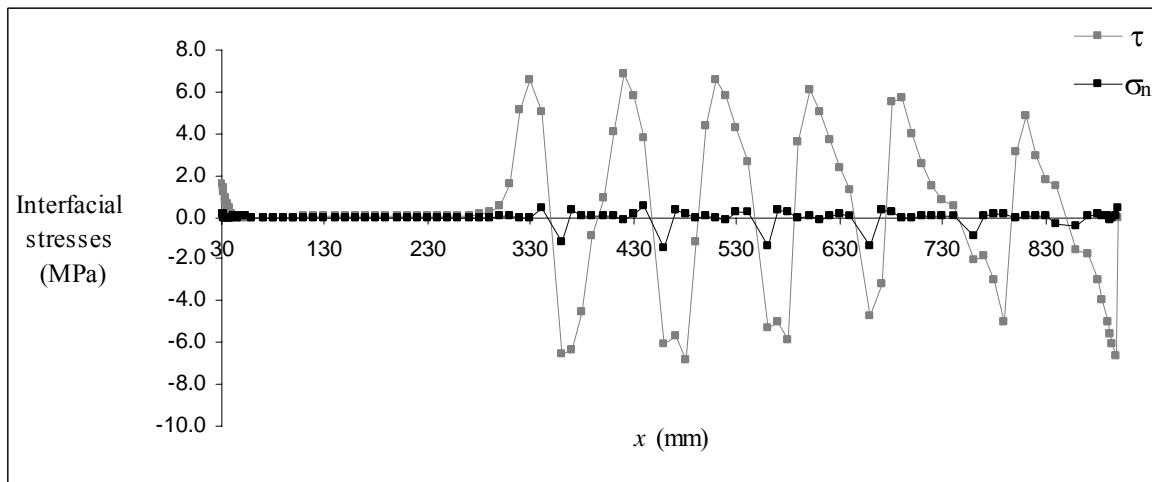


Figure 19 – Interfacial stresses along the beam with $P=19.1\text{kN}$ (sheet).

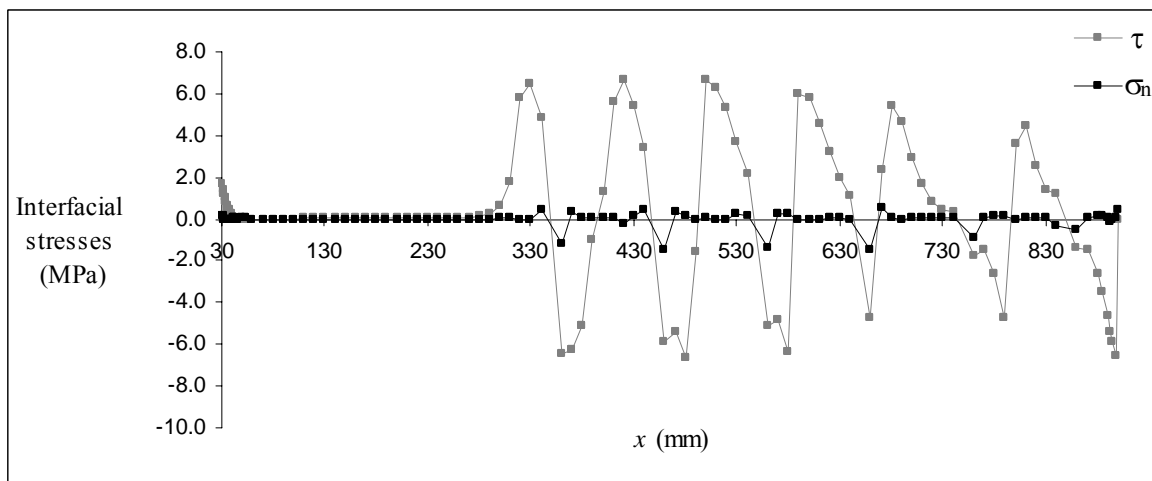


Figure 20 – Interfacial stresses along the beam with $P=20.0\text{kN}$ (sheet).

The smaller stress concentration found in the sheet end of the beam (Figure 21b)) may be due to the fact that the sheet composite thickness is smaller than FRP laminate. Once again

the local failure mode due to stress concentration at the FRP end is not important, as mentioned above; it depends mainly on the flexural rigidity of the FRP cross section. Naturally, once again the debonding due to flexural cracks of concrete is the determinant failure mode.

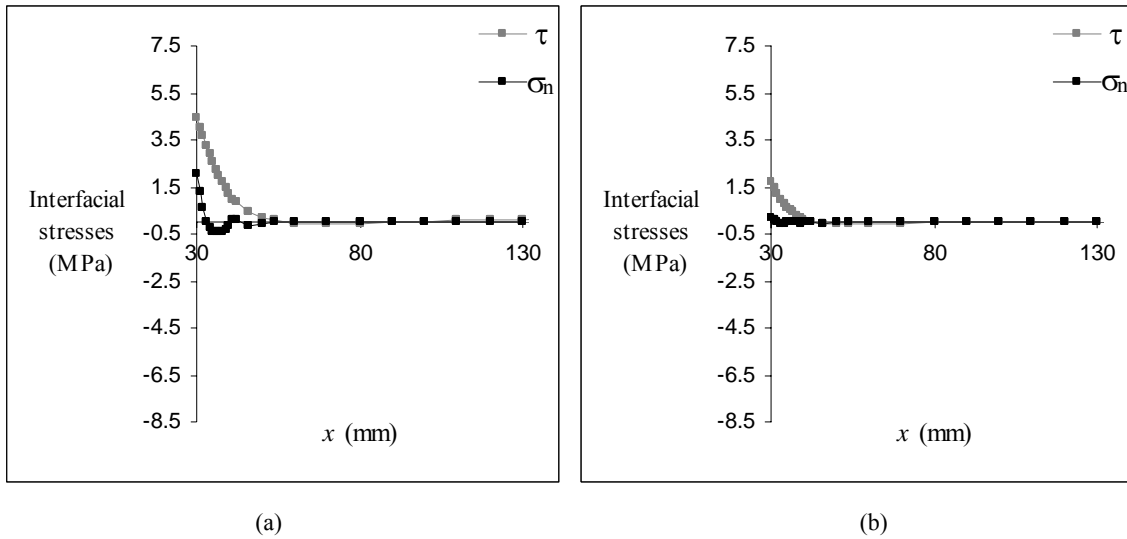


Figure 21 – Detail of the interfacial stresses in the extremity of the FRP laminate (a) and sheet (b).

From Figure 8 to Figure 13 and from Figure 15 to Figure 20 can be observed that peeling stresses are of few importance along the beam span due to concrete cracks. Niu et al. [9] admitted in their work the possibility that only mode-II fracture was taking place. Thus, the methodology presented in Neto (2003) [16] is applied, based on the rectangular simplified diagram method considering a bond-slip model. The maximum load is about 80% and 87% of the theoretical value for laminate and sheet, respectively. In accordance with the above mentioned work, the theoretical value of the maximum load is, in general, smaller than the real value. Thus, it is possible to conclude that mode-II fracture is important in beams reinforced with FRP, because, in general, the thickness considered is smaller. Applying this model [16] to the beam without external reinforcement, it is found that the maximum theoretical and experimental loads perfectly match.

In order to analyze the importance of mode-II fracture in the behavior of the flexural element, in the case of the RC beam strengthened with FRP sheet, a value of $G_F^{II}=0.5\text{N/mm}$ is considered. The structure response is presented in Figure 14. It is noticed that the values of the load are lower and the solution closer to the experimental one, specially in the last part of the curve. In this case the above-mentioned stress interaction is smaller because the bond length is about 47mm [16, 19], as it can be seen from Figure 22 to Figure 25. Thus, a lower maximum load value is expected. According to Niu et al. [9], when stress interaction is present, larger maximum load values are expected, as obtained in the present study. These authors refer that complete debonding does not mean final debonding failure [9]. Thus, the shear stresses interaction can be a favorable effect. However, comparing these two study cases, in which fracture energy values equal to 1.5N/mm and 0.5N/mm are adopted, it is observed that the difference between structural responses is small. Based on the result presented in Figure 14, it is not possible to conclude that $G_F^{II}=0.5\text{N/mm}$ is the most appropriate value in this case. Fracture energy of concrete in mode-II is the material parameter which affects most the maximum load in shear tests [16]. However, in the flexural model, there are other parameters that influence significantly the structure response. The beam's strength depends also on the compressive strength and on the internal reinforcement. Thus, for a given variation of the

maximum load in the FRP a smaller variation of the beam's maximum load is obtained. On the other hand, the explicit integration option leads to more rigid solutions.

From the studied models it is possible to notice that the area of FRP laminate is about the double of the sheet composite area, however the ratio between maximum loads is approximately equal to one. Thus, in spite of different mechanical properties and shear stress interaction, it seems that, whenever possible, it is preferable to increase the width instead of the thickness of the CFRP, similar to the conclusions obtained in previous works [11, 16]. Moreover, more layers are more difficult to execute.

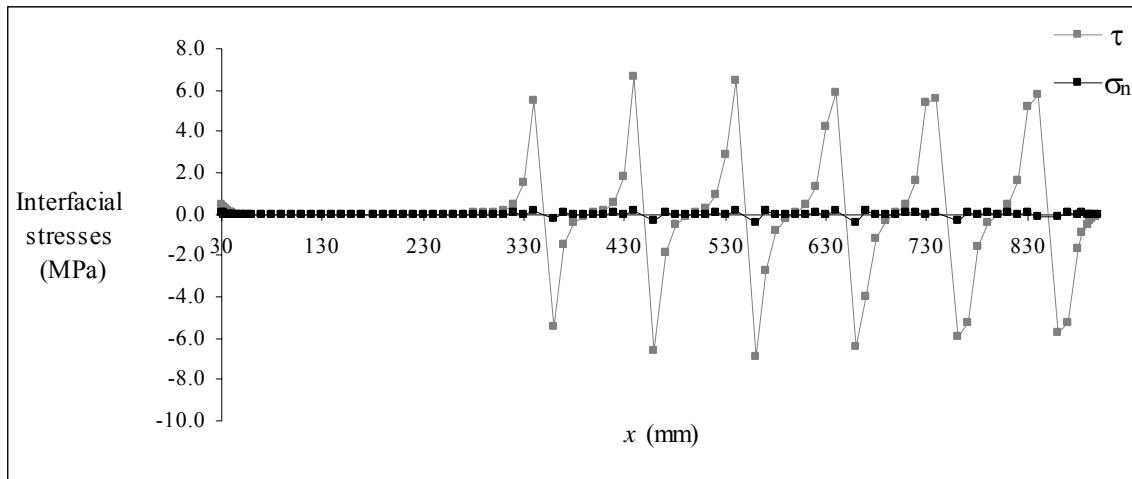


Figure 22 – Interfacial stresses along the beam with $P=4.8\text{kN}$ (sheet – $G_F^{II}=0.5\text{N/mm}$).

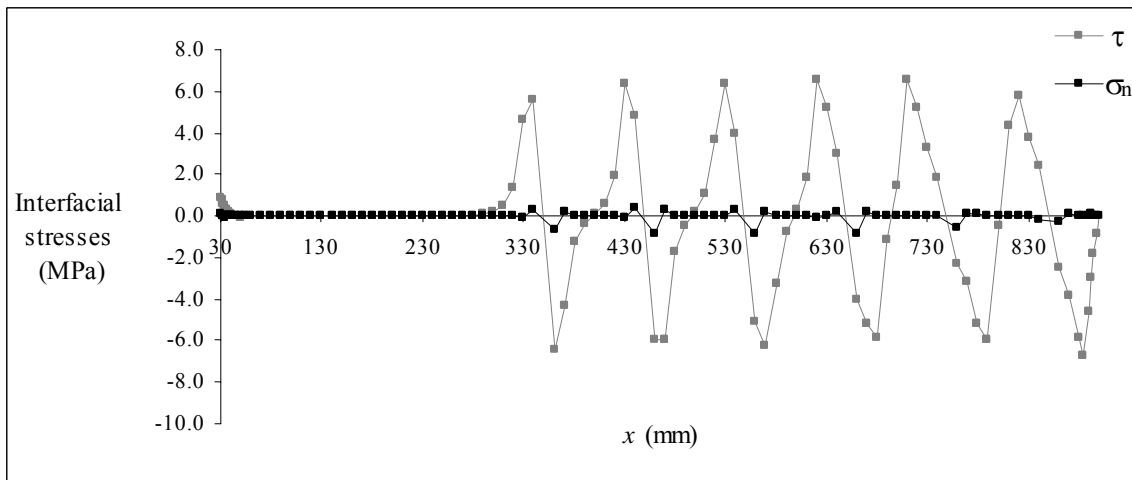


Figure 23 – Interfacial stresses along the beam with $P=10.2\text{kN}$ (sheet – $G_F^{II}=0.5\text{N/mm}$).

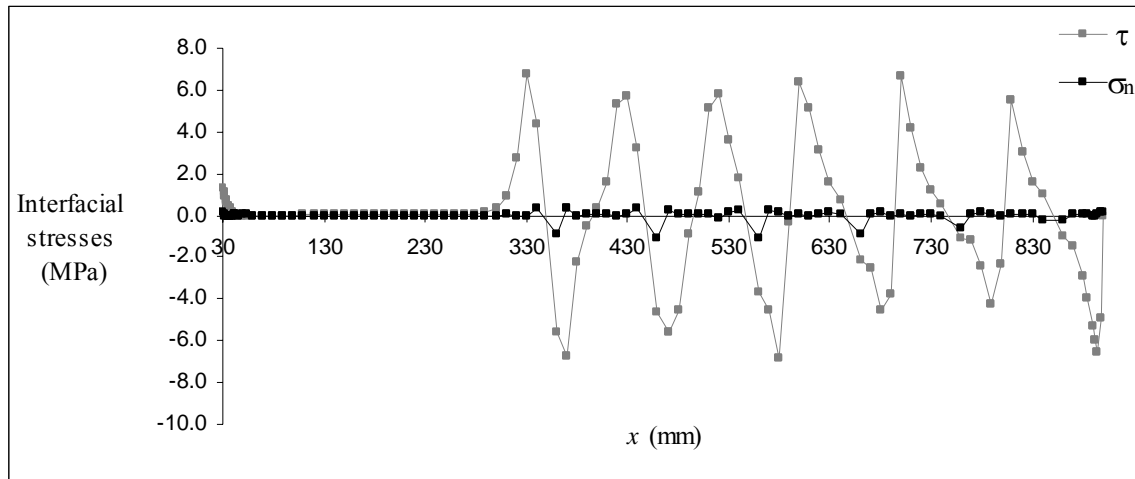


Figure 24 – Interfacial stresses along the beam with $P=15.0\text{kN}$ (sheet – $G_F^{II}=0.5\text{N/mm}$).

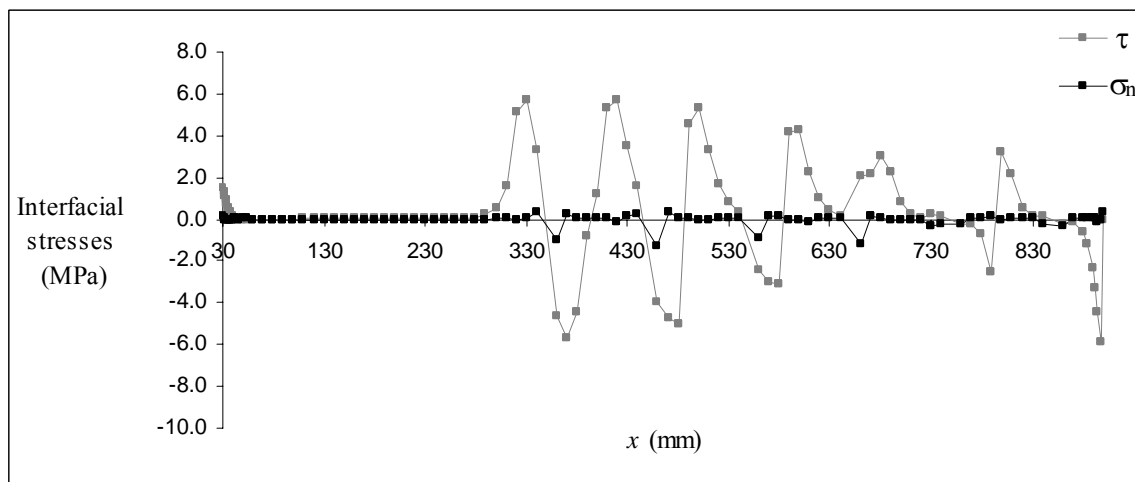


Figure 25 – Interfacial stresses along the beam with $P=18.0\text{kN}$ (sheet – $G_F^{II}=0.5\text{N/mm}$).

4 CONCLUSIONS

- The research focuses on the computational modelling, based on non-linear fracture mechanics, of the stress distribution in the FRP-concrete interface at the composite end and along the beam span of a bending structural element.
- The material properties used in the characterization of the interface behavior, are (in general): the shear and peeling stiffness, the cohesion, the tensile strength and the fracture energy in modes I and II.
- The constitutive behavior adopted for interface elements to model the connection between concrete and internal reinforcement was taken into account and the material model adopted is found to be adequate.
- The consideration of a bond-slip relationship, between concrete and internal reinforcement, allows a good agreement between numerical and experimental results from the beginning of the beam response. However, in terms of the ultimate response, the obtained results, considering perfect bond, are the same with lower calculation times.

- In the FRP end, the shear stress distribution is observed to be similar to the one obtained in a pure shear model and normal stresses to the interface appear. These peeling stresses are first tensile in a small length, changing into compressive stresses and almost vanishing in a length of approximately 10mm.
- The stress concentration noticed in the composite end of the beam is found to play a non important role in the global behavior of the beam; in fact, the composite thickness is less than adequate to mobilize peeling stresses capable of leading to failure.
- The importance of stress concentration at the FRP end depends on the flexural rigidity of the FRP cross section.
- The peeling stresses are important only at the extremity of the CFRP. Since the debonding due to flexural cracks of concrete is the determinant failure mode, the mode-II of fracture energy is an important parameter.
- The methodologies presented in the FIB report 14 [20] only consider the mode-II of fracture, which is adapted to the general cases with FRP reinforcement, taking into account the small thickness adopted.
- The importance of the stress concentration in the failure of the bending beam seems related to the higher thickness of the reinforcement, and this is why mechanisms of anchorage are adopted when metal plates are used.
- A shear stresses interaction can be noted between cracks. This stress interaction occurs when the crack spacing does not exceed significantly the bond length associated to the maximum force in the composite, at two adjacent cracks, obtained in a single shear test.
- From the studied models it seems that, whenever possible, it is preferable to increase the width instead of the thickness of the CFRP.
- Comparing numerical and experimental results it is possible to conclude that the adopted numerical model is adequate. However, the incremental-iterative process needs to be revised with respect to the convergence of the method.

REFERENCES

- [1] A.M. Malek, H. Saadatmanesh, R. E. Mohammad, Prediction of failure load of RC beams strengthened with FRP plate due to stress concentration at the plate end, *Structural Journal*, ACI, **95(2)**, 142-152, 1998.
- [2] Z.S. Wu and H.D. Niu, Shear transfer along FRP-concrete interface in flexural members, *Journal of Material, Concrete Structures and Pavements*, JSCE, **49(662)**, 231-245, 2000.
- [3] O. Rabinovich and Y. Frostig, Closed-form high-order analysis of RC beams strengthened with FRP strips, *Journal of Composites for Construction*, ASCE, **4(2)**, 65-74, 2000.
- [4] B. Täljsten, *Plate bonding – strengthening of existing concrete structures with epoxy bonded plates of steel or fiber reinforced plastics*, Doctoral Thesis, Division of Structural Engineering, Lulea University of Technology, 1994.
- [5] Z.P. Bazant and P.A. Pfeiffer, Shear fracture tests of concrete, *Materials and Structures*, **19**, 111-121, 1986.

- [6] J. Ozbolt, H.W. Reinhardt and S. Xu, Numerical studies of the double-edge notched mode-II geometry, H. Mihashi and K. Rokugo eds. *FRAMCOS-3*, **2**, 773-782, Japan, 1998.
- [7] J. Alfaiate and E.B. Pires, Mode-I and mixed-mode non-prescribed discrete crack propagation in concrete, H. Mihashi and K. Rokugo eds. *FRAMCOS-3*, **2**, 739-748, Japan, 1998.
- [8] J.C. Gálvez, D.A. Cendón, J. Planas, G.V. Guinea and M. Elices, Fracture of concrete under mixed loading - experimental results and numerical prediction, H. Mihashi and K. Rokugo eds. *FRAMCOS-3*, **2**, 729-738, Japan, 1998.
- [9] H.D. Niu and Z.S. Wu, Interfacial debonding mechanism influenced by flexural cracks in FRP-strengthened beams, *Journal of Structural Engineering*, JSCE, **47A**, 1277-1288, 2001.
- [10] P. Neto, J. Alfaiate, J.R. Almeida and E.B. Pires, The influence of mode-II fracture on concrete strengthened with CFRP, *Computers & Structures*, **82(17-19)**, 1495-1502, 2004.
- [11] P. Neto, J. Vinagre and J. Alfaiate, Modeling the behavior of the bonding of fiber reinforced concrete at the plate end, *International Symposium Polymers in Concrete, ISPIC* (in press), 2006.
- [12] A. Hillerborg, M. Modeer and P.E. Petersson, Analysis of crack formation and crack growth in concrete by means of fracture mechanics and finite elements, *Cement and Concrete Research*, **6**, 773-782, 1976.
- [13] S. Dias, L. Juvandes and J. Figueiras, *Comportamento experimental de vigas de betão armado reforçadas à flexão com sistemas compósitos de CFRP do tipo Mbrace*, relatório técnico, LABEST, Faculdade e Engenharia da Universidade do Porto, 2002.
- [14] P.B. Lourenço, and J.G. Rots, A multi-surface interface model for the analysis of masonry structures, *Journal of Engineering Mechanics*, ASCE, **123(7)**, 660-668, 1997.
- [15] J. Alfaiate, J.R. Almeida, Crack Evolution in Confined Masonry Walls, S.R. Idelshon, E. Oñate and E. Dvorkin eds. *Computational Mechanics: New Trends and Applications*, CIMNE, Barcelona, Spain, 1998.
- [16] P. Neto, *Estudo numérico da ligação betão-CFRP*, MSc. Thesis (in press), Instituto Superior Técnico, Universidade Técnica de Lisboa, 2003.
- [17] R. Costa, *Modelação de vigas de betão armado reforçadas com chapas metálicas*, MSc. Thesis (in press), Instituto Superior Técnico, Universidade Técnica de Lisboa, 2005.
- [18] CEB-FIP Model Code 1990, *Design Code*, Comité Euro International du Béton, 1993.
- [19] H. Yuan; Z.S. Wu and H. Yoshizawa, Theoretical solutions on interfacial stress transfer of externally bonded steel/composite laminates, *Journal of Structural Mechanics and Earthquake Engineering*, JSCE, **nº 675/I-55**, 27-39, 2001.
- [20] FIB (CEB-FIP), *Technical report on the design and use of externally bonded fiber reinforced polymer reinforcement (FRP EBR) for reinforced concrete structures - externally bonded FRP reinforcement for RC structures*. Fédération Internationale du Béton, Bulletin 14, 2001.